PHOTOTHERMAL THERAPY AS AN ALTERNATIVE CANCER TREATMENT WITH TOP-DOWN AND BOTTOM-UP GRAPHENE QUANTUM DOTS

by

Gretel Stokes

Submitted in partial fulfillment of the
requirements for Departmental Honors in
the Department of Physics & Astronomy
Texas Christian University
Fort Worth, Texas

December 12, 2022

PHOTOTHERMAL THERAPY AS AN ALTERNATIVE CANCER TREATMENT WITH TOP-DOWN AND BOTTOM-UP GRAPHENE QUANTUM DOTS

Project Approved:

Supervising Professor: Dr. Anton V. Naumov, Ph.D

Department of Physics & Astronomy

Dr. Zygmunt (Karol) Gryczynski, Ph.D

Department of Physics & Astronomy

Dr. Eric E. Simanek, Ph.D

Department of Chemistry

ABSTRACT

Many current cancer treatment options cause various side effects due to the harm they inflict on surrounding healthy tissue. Photothermal therapy provides an alternative form of cancer treatment with reduced side effects. In photothermal therapy, near-infrared light is used to heat up near-infrared absorbing materials that are localized to cancerous tissue to biologically detrimental temperatures. These materials must be biocompatible and able to produce enough heat to kill cancerous tissue when irradiated with infrared light.

In this work, two near-infrared-absorbing materials, termed photothermal agents, are synthesized: reduced graphene oxide quantum dots and hyaluronic acid doped graphene quantum dots. These were determined to be relatively biocompatible by MTT assay. Solutions containing these quantum dots were irradiated with near-infrared light for 45 minutes. Both solutions heated from biological temperature (37 °C) to temperatures above 46 °C, while a solution of deionized water, irradiated as a control, had a temperature increase of only 0.5 °C during the 45 minutes. Additionally, *in vitro* studies of these materials demonstrated their ability to induce hyperthermia in cancer cells upon ten minutes of low-energy laser ablation. HeLa cells treated with solutions of these materials had a reduction in cell viability from above 80% to below 40% following ten minutes of infrared laser irradiation. Overall, reduced graphene quantum dots and hyaluronic acid doped quantum dots were determined to be photothermal agent candidates because of their relative biocompatibilities coupled with efficient production of heat upon irradiation with near-infrared light.

TABLE OF CONTENTS

ACKNOWLEDGEMENTS

I would like to express my gratitude for all the professors who have been foundational in my academic journey at TCU. Dr. Anton Naumov, who has been my research supervisor for three years, has provided patient guidance during this project and others. Working in his lab has given me confidence in myself and an appreciation for scientific research. Additionally, having him as a professor in two semesters of classes instilled in me enthusiasm for the subject of physics, as he passionately taught all subject material. Dr. Naumov truly cares about the success of his students: within their academic, research, and personal endeavors.

I would also like to thank the remaining two committee members who have guided this project—Dr. Karol Gryczynski and Dr. Eric Simanek. Since my first year at TCU, Dr. Gryczynski has challenged me to deeply understand the world around me by asking thought-provoking questions that could be explained with foundational concepts in physics. His attention to the innerworkings of the world around us has given me a love for the holistic knowledge that study of physics provides. I had the privilege of participating in organic chemistry research throughout this year with Dr. Simanek. His guidance and support has had a great impact on both my final year as an undergraduate at TCU and in the trajectory of my future endeavors in graduate school.

I am sincerely grateful for the four years I spent at TCU and all who guided me during this time.

LIST OF FIGURES

INTRODUCTION

Current Radiation Therapies

Cancer remains one of the deadliest diseases, annually leading to almost ten million deaths worldwide.[1] Most current cancer treatment options cause a plethora of side effects, as they inevitability affect both healthy and cancerous tissue.[2,3] One branch of cancer treatment is radiation therapy, of which the main goal is to deprive cancer cells of their multiplication potential by damaging their DNA.[4] This thesis looks at current modes of radiation therapy and a possible alternative option for radiation with reduced damage to healthy cells.

In the most common form of radiation therapy, high energy electromagnetic waves, such as X-rays or gamma rays, are used to ablate cancer cells. These waves stop cancer cell proliferation and trigger cell-death by depositing energy from their photons in the malignant tissue. They do so by transferring energy to electrons in a process called Compton scattering.[5] Deposited photons either kill the cell directly by degrading DNA or indirectly by forming hydroxyl free radicals when electrons attach onto water molecules contained in the cell (**Figure 1**).

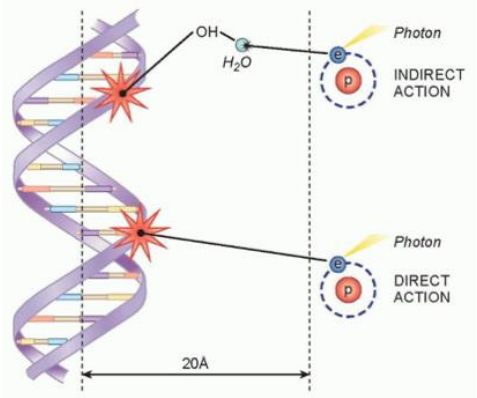

Figure 1. The direct and indirect effects of X-ray and gamma ray radiation on DNA. Incident photons transfer their energy to electrons in a process called Compton scattering. These electrons can damage DNA via direct interaction with it or indirectly by forming hydroxyl free radicals that induce damage. Figure taken from reference #6.

Controlling the site at which energy from external X-ray and gamma ray beams is deposited is difficult. Multiple beams that vary in their entrance sites may be used so that they are superimposed over the cancerous tissue, thus, delivering the maximum dosage there.[7] However, these beams inevitably deposit energy in healthy cells prior to reaching malignant tissue (the entry dosage) and after passing through the cancerous tissue (the exit dosage) (**Figure 2**). The deposition of high levels of energy in non-cancerous tissue can lead to future cancer development in

surrounding sites and local side-effects for patients undergoing high-energy radiation therapies. Thus, cancer-specific radiation treatments are an active area of scientific inquiry.

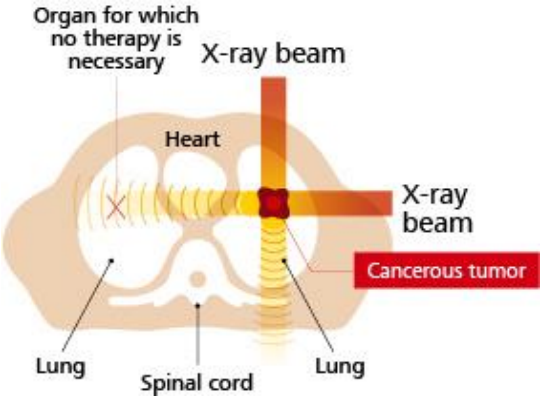

Figure 2. Traditional X-ray radiation therapy. Two beams are used to administer a higher dosage of radiation therapy to the cancerous tissue. However, surrounding tissue is still damaged via the entrance and exit beams. This leads to side effects in patients to whom this therapy is administered. Figure adapted from reference #8.

Photothermal Therapy

One possible alternative to current modes of radiation therapy is called photothermal therapy (PTT). Overall, PTT has low costs, high specificity, and reduced side-effects for normal tissues.[3] Instead of high-energy X-ray or gamma ray radiation sources, photothermal therapy uses near infrared light (wavelength ~1,000 nm)—which is significantly lower in energy—to heat and kill cancer cells. **Figure 3** shows the electromagnetic spectrum for comparison of the energies of X-rays/gamma rays and infrared light. In photothermal therapy, agents that absorb near-infrared light are localized to cancerous tissue. These materials, termed photothermal agents, absorb energy from photons when they are shone with near infrared light and dissipate it in the form of heat to trigger cancer cell death.[2] **Figure 4** shows a schematic for how photothermal therapy works to kill cancer cells.

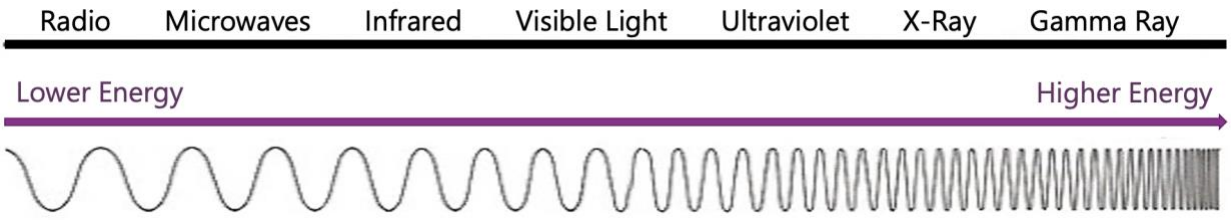

Figure 3. The electromagnetic radiation spectrum. Gamma ray and X-ray radiations have the highest energies, while infrared radiation has lower energy than visible light. Because highly energetic waves interact with and damage biological tissue, gamma rays and X-rays are more damaging to cells than infrared light.

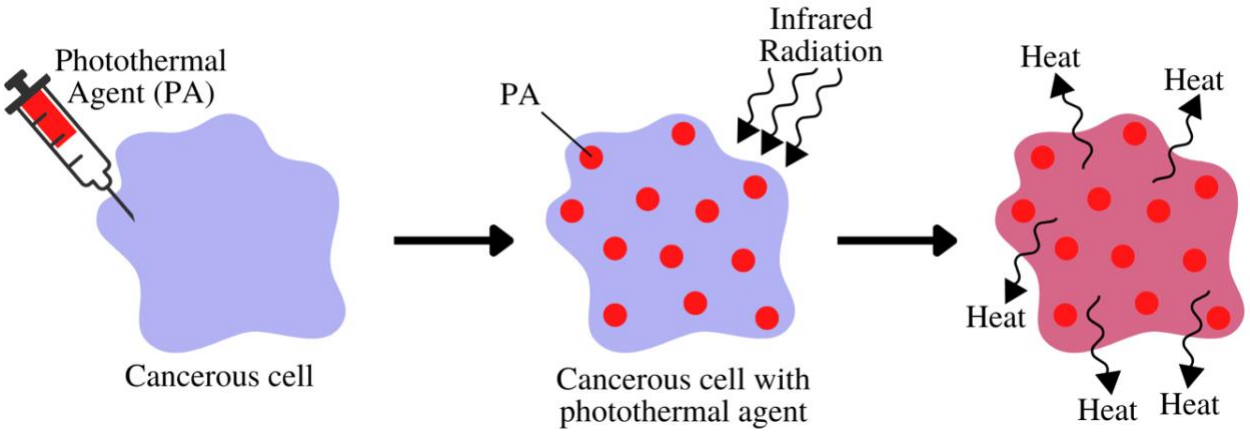

Figure 4. How photothermal therapy kills cancer cells. A photothermal agent is injected into cancerous tissue. Cancerous cells, now containing photothermal agent, are irradiated with near infrared light. The photothermal agent absorbs the infrared radiation and converts it to thermal (heat) energy. This heats the cancerous cells to biologically detrimental temperatures, selectively killing them.

Photothermal therapy may be an effective approach to specifically target cancerous tissue for multiple reasons. First, using a relatively low-energy radiation source—such as near infrared light—reduces surrounding cell damage caused by the entrance and exit doses. Additionally, cancer cells are less resistant to elevated temperatures compared to healthy cells due to their compromised DNA-repair mechanisms.[9] DNA repair pathways are commonly mutated in cancers, rendering them more vulnerable to DNA damage caused by radiation therapies.[10] Cell death for cancerous tissue due to PTT is generally accomplished when the cancerous tissue is exposed to temperatures above 42 °C.[11] Thus, photothermal agents must be capable of heating tissues to 42 °C or higher for hyperthermia-induced cancer cell death.

Photothermal therapy has been mostly limited to preclinical studies. Several studies have been done *in vivo*, using mice as a model organism. In one of these, PTT treatment effectively ablated tumors that had been injected with photothermal agent and irradiated with an 808 (near-infrared) nm laser for twenty minutes, daily, over a five-day-period.[12] In the week following treatment, there was no regrowth of tumor. Additionally, there were two control groups: one treated with only the laser (not injected with photothermal agent) and one treated only with photothermal agent (not irradiated with the laser). Both control groups experienced rapid tumor growth over the testing period. Thus, this study indicates PTT alone could be an effective cancer treatment. Another *in vivo* study established that PTT could be used as an adjuvant therapy following breast-conserving surgery to reduce the risk of local cancer recurrence.[13] In addition to these *in vivo* studies demonstrating the efficacy of PTT as an effective cancer treatment, many studies of photothermal therapy largely focus on the development of efficient photothermal agents.[14]

Additionally, a few clinical trials have demonstrated PTT as an effective cancer treatment. In a 2019 phase I clinical trial using photothermal therapy to treat prostate cancer, optical fibers that emitted near-infrared light and near-infrared-absorbing gold nanoparticles were placed in 19 patients at the site of cancer. Of these 19 people, 94% of patients had tumors that were successfully ablated with no serious complications and no marked change in symptom score.[14] Overall, PTT may offer an effective mode of radiation therapy with fewer side effects than traditional therapies.

Photothermal Agents

For PTT to transition to clinical application, biocompatible photothermal agents capable of heating cancerous tissues to temperatures above 42 °C upon near-infrared irradiation must be identified. Efficient photothermal agents must have certain absorptive qualities: high levels of light absorption at the wavelength of light used for treatment and a high photothermal conversion efficiency, or the ability to convert absorbed light to heat.[14] Additionally, they must be minimally toxic to surrounding healthy tissue and have good biocompatibility.[14] Potential photothermal agents can be classified into several types: organic dye molecules, organic nanoparticles, gold nanomaterials, carbon-based materials, and inorganic nanomaterials (**Figure 5**).[11,14] Among these agents, organic materials are often relatively biocompatible; however, they have limitations such as low photothermal conversion efficiency. Inorganic and noble metal materials usually have the opposite properties: low biocompatibility and high photothermal conversion efficiency.[11] Some carbon-based nanomaterials may offer a combination of high photothermal conversion efficiency and biocompatibility.

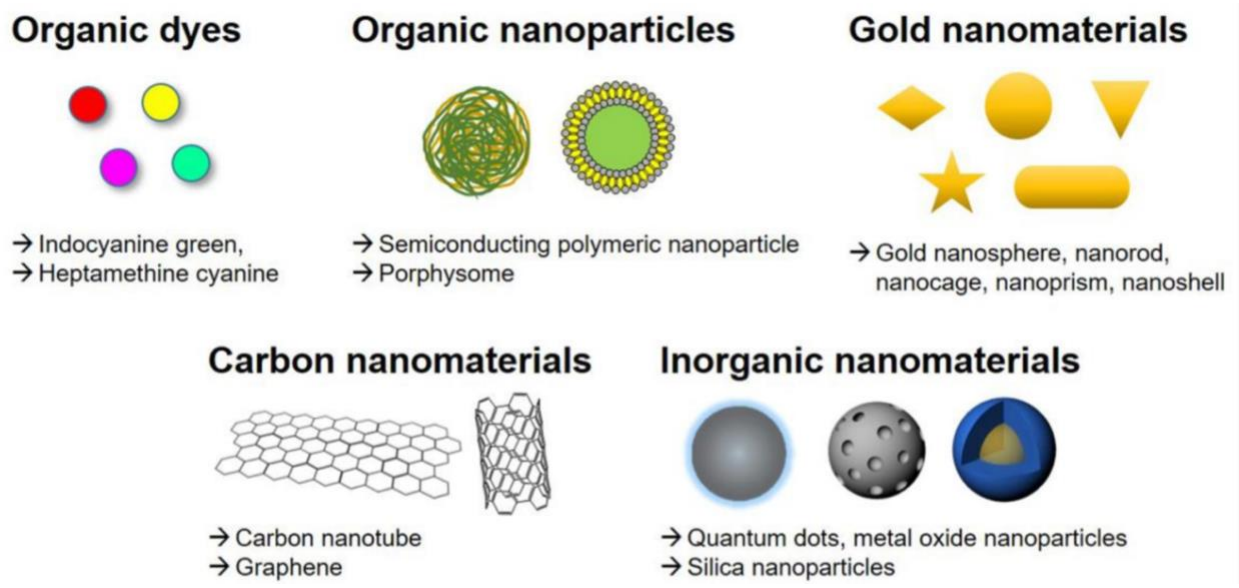

Figure 5. Classes of potential photothermal agents. Figure taken from reference #11.

Generally, nanosized (between 1 and 100 nm in diameter) photothermal agents achieve higher photothermal conversion efficiency than small-molecule agents.[11] Additionally, nanoparticles accumulate at tumor sites due to the enhanced permeability and retention effect: a large concentration of nanoparticles passively accumulates at tumor sites because they are small enough to enter via leaky vasculature endogenous to cancerous tissue.[15] Traditionally, research on nanosized materials has focused on noble metal and semiconductor nanoparticles as photothermal agents, which usually have high cytotoxicity.[11] However, recently there has been an emphasis on developing nanoparticles with lowered cytotoxicity.

A possible avenue of biocompatible nanoparticle development is carbon-based nanomaterials. Carbon-based nanomaterials have become a focus of nanoparticle research since they were first observed in 1991.[16] Carbon nanomaterials are a diverse species with various structures, functionalization, and biomedical applications. **Figure 6** provides a depiction of several prominent carbon-based nanomaterials. Out of these, carbon nanotubes and graphene-based nanoparticles have attracted attention as possible PTT agent candidates due to their high optical absorption in the NIR region and high surface area.[11] However, carbon nanotubes have limited clinical applications because they have high accumulation in tissue and a long excretion time (more than 7 days).[17] Graphene-based nanomaterials have shown low cytotoxicity and high photothermal conversion efficiency in several studies.[14,18-21] Thus, graphene-based nanomaterials are candidates for efficient PTT agents.

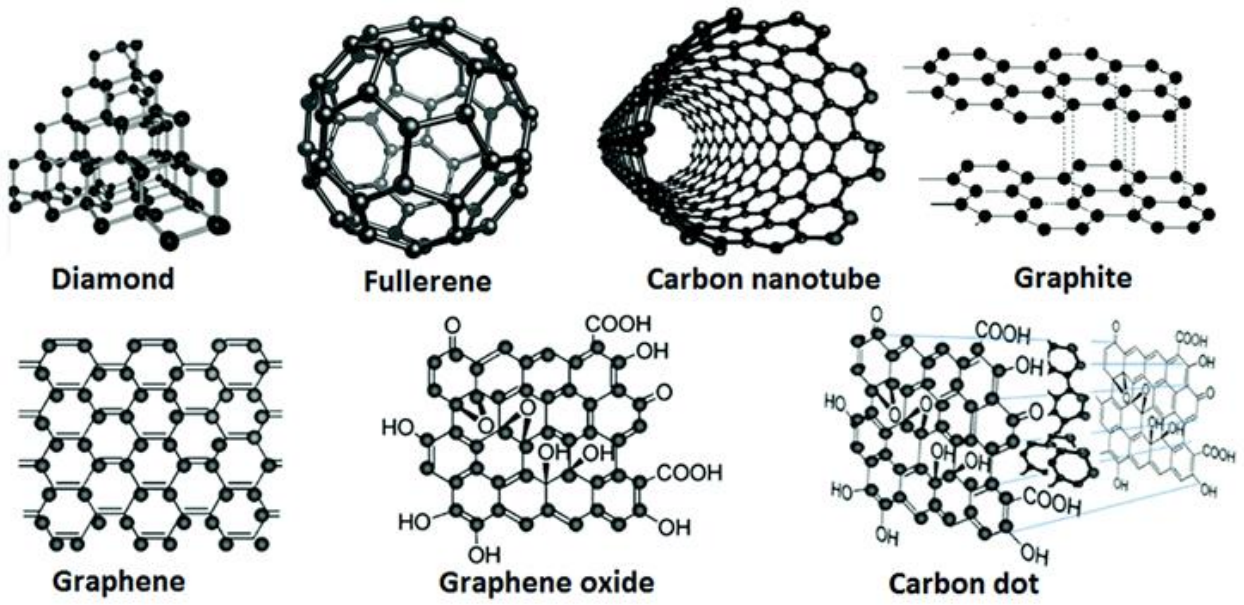

Figure 6. Various carbon-based nanoparticle structures. Carbon nanomaterials are highly diverse and offer many biomedical applications based on their specific properties. Figure taken from reference #22.

Graphene Quantum Dots as Photothermal Agents

Herein, graphene and its derivatives are explored as possible photothermal agents. Graphene is an allotrope of carbon made up of a flat, honeycomb structure of sp^2-hybridized carbons. Oxidation of graphene gives rise to graphene oxide, which is a heavily oxygenated derivative of graphene. Reduction of graphene oxide results in reduced graphene oxide, which has less oxygen-functionalization. The process of converting graphene into its two derivatives is shown in **Figure 7**. Doping the surface of graphene with oxygen-containing groups allows for it to be functionalized with other molecules, which can be useful for cancer-targeting applications and increasing biocompatibility.[23] The higher level of functionalization in graphene oxide than reduced graphene oxide decreases its capability as a thermal conductor, which lowers its photothermal conversion efficiency.[24] Reduced graphene oxide is an allotrope of carbon that offers facile functionalization, unlike pure graphene, and a higher photothermal conversion efficiency than graphene oxide. Thus, reduced graphene oxide is a better candidate as a photothermal agent than are graphene and graphene oxide.

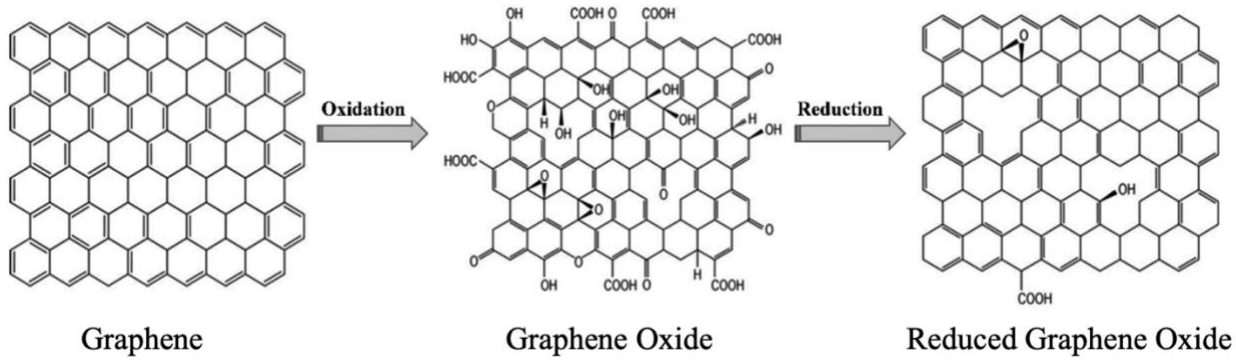

Figure 7. Functionalization of graphene with oxygen-containing groups. Graphene can be oxidized to give graphene oxide, which can be reduced to produce reduced graphene oxide. Figure adapted from reference #25.

Quantum dots, which are a class of nanoparticles considered to be zero dimensional due to their small size (typically between two and ten nanometers), exhibit interesting absorptive properties. This is mostly because they exhibit the quantum confinement effect.[26] The quantum confinement effect is a phenomenon in which an electron confined to a space only a few nanometers in dimension experiences a broadening of the possible energy levels that it can occupy. This is due to the Heisenberg uncertainty principle: that both the position and speed of a particle cannot be known with perfect accuracy.[26-28] Reduced graphene oxide can be used to prepare reduced graphene oxide quantum dots. Reduced graphene oxide quantum dots are single sheets of reduced graphene oxide with lateral dimensions below ten nm. A representative structure of a reduced graphene oxide quantum dot is given in **Figure 8**. These frameworks combine the thermal

conduction properties of reduced graphene oxide with the absorptive properties generally attributed to zero-dimensional quantum dots.

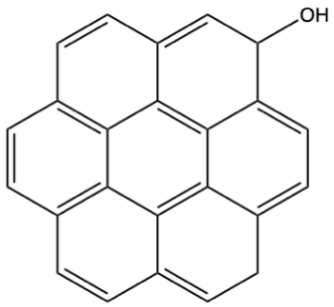

Figure 8. Representative structure of a reduced graphene oxide quantum dot. Functionalization with a hydroxyl (OH) group is shown. However, reduced graphene oxide quantum dots prepared from reduced graphene oxide frequently have methyl, epoxide, and carboxylic acid functional groups, as well. These quantum dots are not heavily functionalized with oxygen-containing groups, as reduced graphene oxide quantum dots are more reduced than graphene oxide quantum dots.

Additionally, graphene quantum dots have been shown to have reduced cytotoxicity as compared with other carbon-based nanomaterials. One study following functionalized graphene quantum dot degradation and excretion determined that by 32 hours quantum dots are fully or partially degraded.[2] Graphene-based quantum dots have faster degradation and excretion following internalization than many other carbon-based nanostructures. This limits their off-target accumulation and damage to healthy cells, which has been a barrier for other carbon-based nanomaterials to transition to widespread clinical use. Additionally, previous studies have shown that reduced graphene oxide quantum dots have high biocompatibility—unlike their reduced graphene oxide parent material.[29] Thus, reduced graphene oxide quantum dots and functionalized graphene oxide quantum dots are strong candidates for PTT agents, as they are biocompatible and have several properties that increase their photothermal conversion efficiency.

This study characterizes the potential of two derivatives of graphene quantum dots—reduced graphene oxide quantum dots and hyaluronic acid doped graphene quantum dots—as photothermal agents. The reduced oxide graphene quantum dots (RGQDs) have a scalable synthesis, exhibit NIR absorbance, and are highly biocompatible.[26] The other characterized graphene quantum dots are doped with hyaluronic acid (HA). Hyaluronic acid is an acidic mucopolysaccharide whose backbone is endowed with tumor targeting parts that specifically recognize CD-44, a surface adhesion receptor that is highly expressed in many cancers and involved in cancer cell dissemination and metastasis.[30] **Figure 9** gives the structure of hyaluronic acid. Therefore, HA-doped architectures can potentially specifically target cancer cells that exhibit this upregulation of CD-44 receptors.

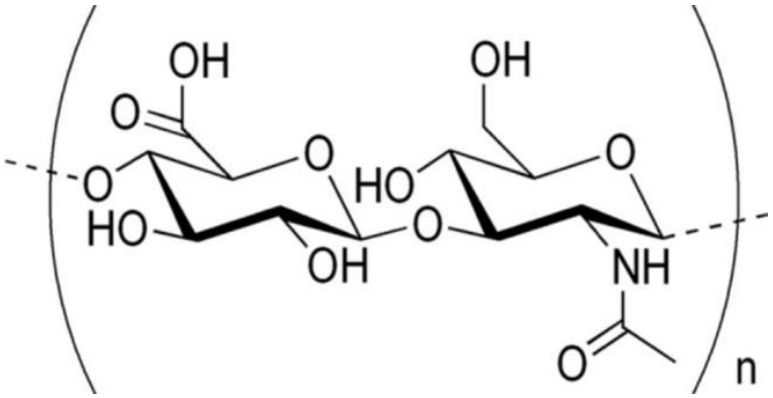

Figure 9. Hyaluronic acid structure. Figure taken from reference #31.

The two samples of quantum dots are synthesized via different approaches. For RGQDs, a top-down synthetic method is applied: a larger material is chemically cut down to the size of quantum dots (~5 nm). In the second synthetic approach, a bottom-up method is used to prepare hyaluronic acid-doped graphene quantum dots: quantum dots are prepared from joining of basic units. This paper describes RGQDs and HA doped graphene quantum dots (HA-GQDs), synthesized via a top down and bottom-up approach, respectively, as effective agents for photothermal therapy.

EXPERIMENTAL

Chemicals and Materials

Reduced Graphene Oxide Quantum Dots. RGQDs were prepared from reduced graphene oxide, purchased from Graphene Supermarket (SKU: HP-RGO-025G). The reduced graphene oxide particles that were purchased for use in the synthesis of RGQDs were in monolayers with lateral sizes between three and ten microns. The RGQDs were synthesized via a top-down approach by chemically cutting reduced graphene oxide into smaller pieces to obtain quantum-dot-sized materials. Chemical scission was achieved via oxidation of the reduced graphene oxide using sodium hypochlorite. A solution of sodium hypochlorite, which is commonly known as bleach, was purchased from LabChem (SKU: LC246304, 5% w/v). The products were purified with dialysis using a 1 kDa dialysis bag (Repligen, SKU: 132104).

Hyaluronic Acid Graphene Quantum Dots. Hyaluronic acid quantum dots were prepared via a bottom-up approach: a larger structure was assembled from basic units. The precursor material used as a building block for HA-GQDs was a powdered sample of 5 kDa hyaluronic acid (HA5K-5), purchased from Lifecore Biomedical. The samples were centrifuged to purify with a HighSpeed™ Microcentrifuge purchased from Southwest Science (SKU: SC1024).

Methods

General Methods. Transmission electron microscopy (TEM, JEOL JEM-2100, MA, USA) with energy dispersive X-ray analysis (EDX, JEOL, MA, USA) was used on a carbon-coated 200 mesh copper grid (Electron Microscopy Sciences, CF300-CU, PA, USA) on which samples were air-dried. A discussion on TEM and EDX follows in the "Instrumentation" section.

Top-Down Synthesis of Reduced Graphene Oxide Quantum Dots. RGQDs were synthesized via a top-down approach by oxidation and scission of high porosity reduced graphene oxide. Reduced graphene oxide was dispersed in deionized (DI) water at a concentration of 0.25 mg/mL. Sodium hypochlorite (1 mL, 5% w/v) was added into the aqueous reduced graphene oxide suspension. The vials were shaken, capped, and allowed to react in the dark for two days. The products were purified via dialysis in DI water for 24 hours. The water was changed every 30 minutes during the first 3 hours and every 7 hours for the remaining time. The solution was passed through a 0.22 μm syringe filter to remove any unreacted reduced graphene oxide.

Bottom-Up Hylauranic Acid Doped Graphene Oxide Quantum Dots. The powdered sample of hyaluronic acid was heated to 300 °C for five minutes on a hot plate. After cooling to room temperature, the sample was centrifuged, and the precipitate was discarded. The supernatant was further centrifuged with a 10 kDa centrifugation filter to remove unreacted hyaluronic acid. The solution was passed through a 0.22 μm syringe for additional purification.

Cell Culture. HeLa cells were utilized for *in vitro* studies. These cells were cultured using complete medium consisting of DMEM (D6046, Sigma-Aldrich, MO, USA) supplemented with 10% FBS (16140-063, Gibco, Dublin, Ireland), L-Glutamine (G7513, Sigma-Aldrich, MO, USA), non-essential amino acid solution (M7145, Sigma-Aldrich, MO, USA), and 1% penicillin/streptomycin (P4333, Sigma-Aldrich, MO, USA). The cell culture was held in an incubator at 37 °C with 5% CO_2 (Midi CO_2, Thermo Scientific, MA, USA).

Cell Viability MTT Assay. To assess the biocompatibility of the RGQDs and HA-GQDs, an MTT (3-(4–dimethylthiazol-2-yl)-2,5 diphenyltetrazolium bromide) assay (Invitrogen M6494, Thermo Fischer Scientific, MA, USA) was performed. Into each well on a 96-well plate, 5,000 cells per 200 μL were seeded and held in the incubator. After 24 hours of incubation, complete medium in the 96 well plate was replaced with 100 μL of 1 mg/mL of MTT and stored in the incubator for four hours. The MTT was replaced with 100 μL of DMSO and placed on an orbital shaker for 5 minutes prior to absorption measurements from a plate reader (μQuant, BioTek Instruments, VT, USA).

Photothermal Conversion Characterization. To characterize the photothermal effect of the prepared graphene quantum dots, separately, 3 mL of aqueous RGQDs at 1.5 mg/mL and HA-GQDs at 1.7 mg/mL (the maximum concentrations with >80% cell viability from MTT assays) were irradiated with a 0.8 W/cm^2 808 nm laser (808MD-12V-BL, Q-BAIHE, China) for 45 minutes. DI water was irradiated as a control. These experiments were performed in an oven, held at biological temperature (37 °C), while the suspensions were magnetically stirred. Temperature measurements were taken every fifteen seconds with a K-type thermocouple, whose temperature probe was submerged in the solution. Three trials were measured for each material at the given concentrations. **Figure 10** gives a diagram of the experimental set-up.

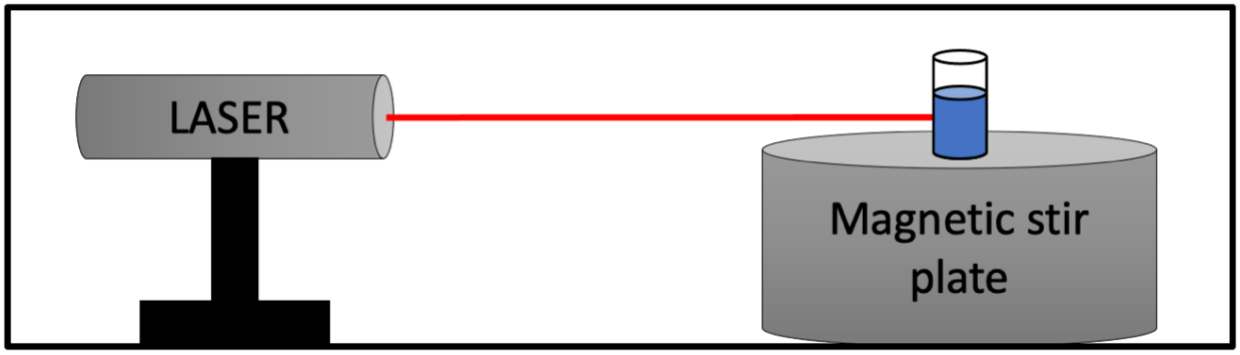

Figure 10. Photothermal conversion characterization experimental set-up. A laser is set to irradiate the given sample for 45 minutes inside an oven held at biological temperature (37 °C).

Automated Laser Irradiation and Temperature Measurement on Cell Cultures Using Synthesized Graphene Quantum Dot Samples as Photothermal Agents. To test the photothermal capability of the synthesized graphene quantum dots *in vitro*, HeLa cells were treated with RGQDs at a concentration of 1.5 mg/mL and HA-GQDs at 1.7 mg/mL for 24 hours. These cells were held at a starting temperature of 37 °C. They were irradiated with a 0.8 W/cm^2 808 nm laser (808MD-12V-BL, Q-BAIHE, China) for zero, one, five, and ten minutes. The temperatures of the cells were recorded following irradiation using a T-type thermocouple (TL0024, Perfect Prime, NY, USA). Additionally, as a control, untreated HeLa cells were irradiated for ten minutes. To assess cell viability, an MTT assay was performed on HeLa cells after laser ablation and temperature measurements. All measurements were automatically taken, using a retrofitted 3D printer (CR-10mini, Creality, Shenzhen, China), equipped with the laser and thermocouple attached to the extruder component of the 3D printer. The 3D printer was placed inside a biosafety hood (Forma 1284, Thermo Fisher Scientific, MA, USA) with a DI water reservoir to maintain the humidity of the biosafety hood environment. An iterative code (written in G-code) was written to set the temperature of the heat bed of the 3D printer to biological temperature (37 °C), position the laser and thermocouple at individual wells, and turn on the laser. A wireless data logger thermometer

software (TC0521, Perfect Prime, NY, USA) was used to collect the temperature measurements acquired by the thermocouple.

Instrumentation

Transmission Electron Microscopy. Transmission electron microscopy (TEM) was used to determine the size and morphologies of the prepared quantum dot samples. In TEM, an electron beam is passed through an ultrathin sample and forms an image on a photographic plate.[32] This provides a direct image of the nanoparticle on an atomic scale. **Figure 12** provides a depiction of how images are produced using TEM.

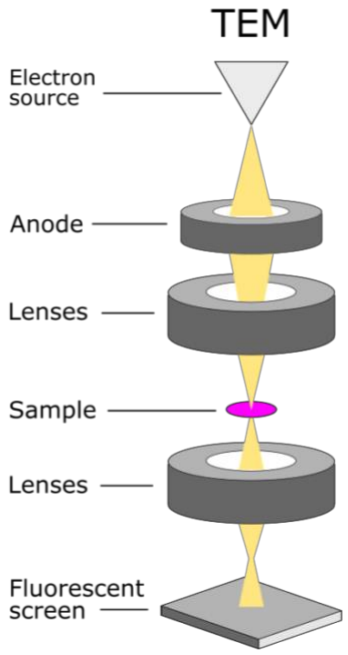

Figure 12. Basic set-up for a transmission electron microscope. Electrons are accelerated as they pass through an anode. Through the lens, they are focused into a beam that passes through a thin layer of sample. The sample interacts with and absorbs the beam. After passing through sample, the beam is focused onto a fluorescent screen, which reads the absorbance pattern of the beam. Figure taken from reference #33.

Energy Dispersive X-ray Spectroscopy. Energy dispersive X-ray (EDX) spectroscopy, which is an analytical method used to determine relative quantities of elements in a sample, was used to characterize the two samples of quantum dots.[34] In EDX, a beam of high energy particles, like protons or electrons, is focused on the sample. When the beam and sample interact, X-rays are emitted. Different elements interacting with the particle beams produce X-rays that are different in energy. These energies are detected and read into a computer, which produces a spectrum with peaks correlating to the different energies of X-rays emitted. The intensity of each spectral peak

corresponds to the relative quantity of a given element in a sample. **Figure 11** shows a diagram of how EDX works to determine the relative abundance of each element present in a sample.

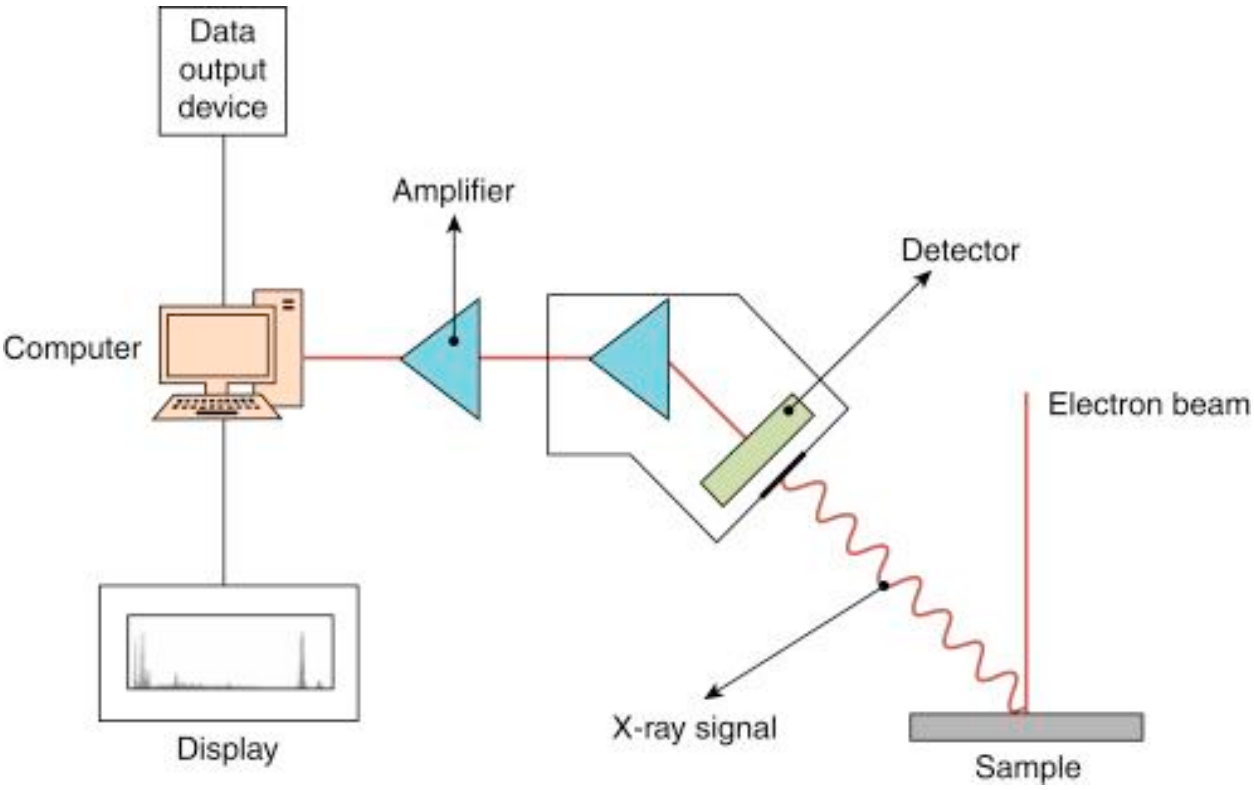

Figure 11. Energy dispersive X-ray spectroscopy. An electron beam is focused on a sample. This beam interacts with elements in the sample to produce X-rays at given energies for each element. The X-rays are detected, amplified, and read into a computer. The computer gives a spectrum with peaks corresponding to different relative abundances of elements in a given sample based on the intensity of different energies of X-rays that reach the detector. Figure taken from reference #34.

RESULTS AND DISCUSSION

Results

Characterization of Graphene Oxide Quantum Dots. The morphologies of the synthesized RGQDs and HA-GQDs were characterized via TEM. The size of RGQDs and HA-GQDs are on the nanometer scale (**Figure 12**). Their size range is what would be expected for quantum dots. Furthermore, both quantum dots have a crystalline structure with an interplanar distance of 0.21 nm, which is characteristic of the lattice spacing in graphene.[35] Additionally, these were characterized via EDX elemental analysis. From the EDX spectroscopy, the synthesized RGQDs were comprised of 91.3% carbon and 8.7% oxygen; the HA-GQDs contained less oxygen functionalization with 98.1% carbon and 1.9% oxygen relative elemental composition. The presence of oxygen functional groups in the quantum dots makes them amenable to

functionalization with other structures.[23] Overall, the TEM images and EDX spectroscopy confirm that the synthesis of oxygen-functionalized graphene quantum dots via a top-down approach (for RGQDs) and a bottom-up approach (HA-GQDs) was successful.

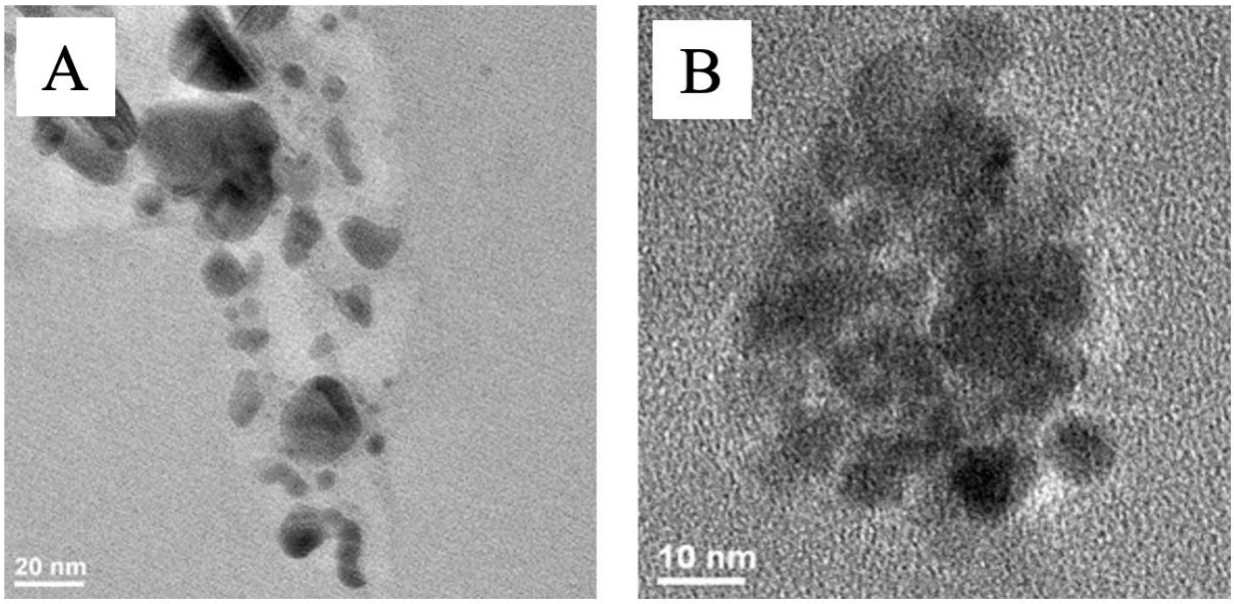

Figure 12. Transmission electron microscopy images of (A) RGQDs and (B) HA-GQDs. These show the sizes of the two quantum dot samples are on the nanometer scale.

Cell Viability Assay. Prior to assessment of the synthesized GQDs as photothermal agents, an MTT assay was performed to assess the biocompatibility of the RGQDs and HA-GQDs. **Figure 13** graphically shows the results of the MTT assay. Measurements of cell viability are given for cells treated with increasing concentrations of GQDs. Cells treated with a concentration of 1.5 mg/mL and 1.7 mg/mL give ~80% viability for RGQDs and HA-GQDs, respectively. Thus, these concentrations were used in following characterizations of the photothermal effect of the synthesized GQD photothermal agents.

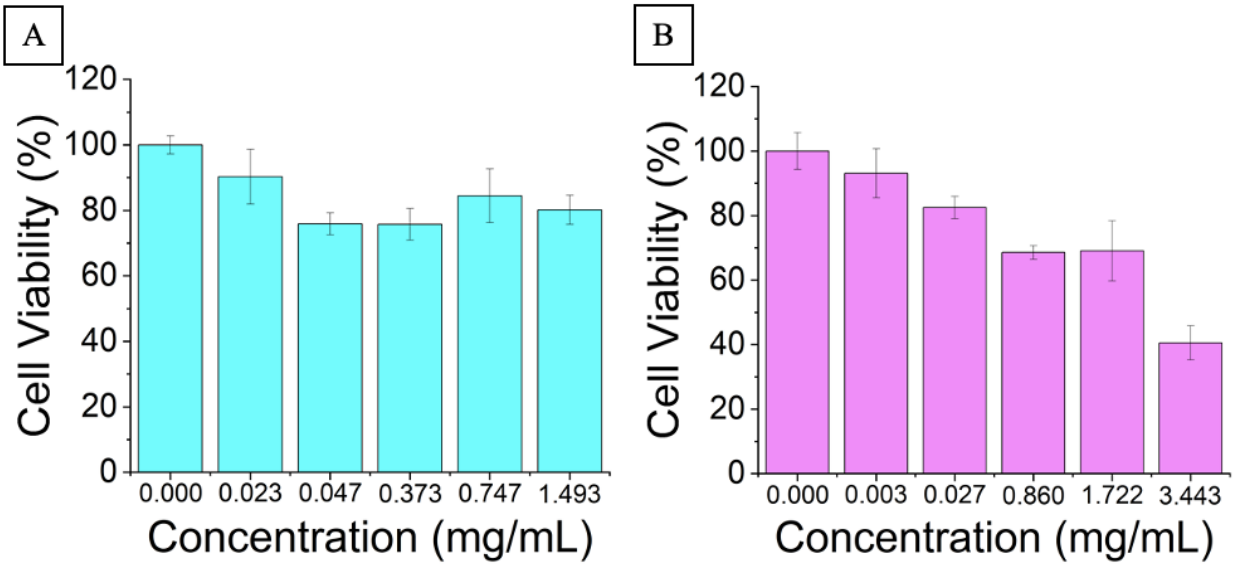

Figure 13. MTT assay of HeLa cells with (A) RGQDs and (B) HA-GQDs. For RGQDs, cell viability remained above 80% at a concentration of 1.49 mg/mL RGQDs; for HA-GQDs, cell viability remained above 80% at a concentration of 1.72 mg/mL HA-GQDs.

Photothermal Conversion Characterization. The photothermal effect of the two synthesized GQDs was measured in aqueous solution in a cuvette at 1.5 mg/mL and 1.7 mg/mL concentrations of RGQDs and HA-GQDs, respectively. In contrast to previously published works, the photothermal effect at biological temperatures is modeled. The temperature measurements show a 10 °C increase for the solution of RGQDs (final measured temperature of 47 °C) and a 9 °C increase in temperature for the solution of HA-GQDs (final measured temperature of 46 °C). A control sample of water was irradiated under the same experimental conditions for 45 minutes. During which time, the water had a 0.5 °C increase in temperature (from an initial temperature of 36.8 °C to 37.3 °C). To ensure their stability as photothermal agents, each sample underwent three cycles of laser irradiation, as indicated by the error bars in **Figure 14**. From this experiment, RGQDs are more stable than HA-GQDs as photothermal agents, as there was less change in collected data over several trials for the RGQDs than the HA-GQDs.

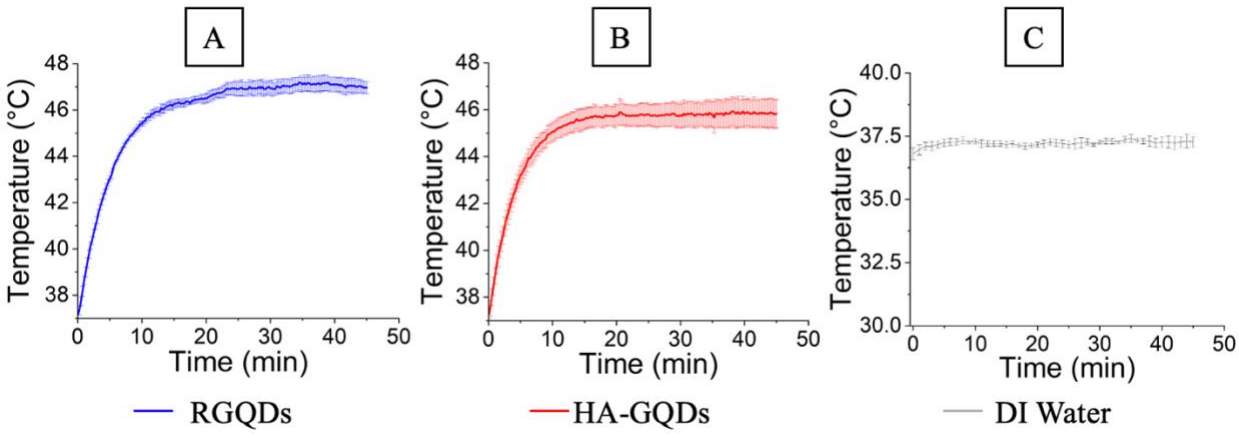

Figure 14. Temperature vs. time of irradiation of (A) RGQDs (1.5 mg/mL) and (B) HA-GQDs (1.7 mg/mL) with a 0.8 W/cm^2 808 nm laser irradiation. Measurements were taken every fifteen seconds over a 45-minute period. The 1.5 mg/mL sample of RGQDs (A) had a change in temperature of 10 °C to a final temperature of 47 °C. The 1.7 mg/mL sample of HA-GQDs (B) had a change in temperature of 9 °C to a final temperature of 46 °C. A pure sample of DI water (C) was irradiated for 45 minutes as a control. The change in temperature for the control was 0.5 °C to a final temperature of 37 °C.

Automated Laser Irradiation and Temperature Measurement on Cell Cultures using synthesized GQDs as the photothermal agent. The results of laser irradiation of the cell cultures treated with RGQDs and HA-GQDs are given in **Figure 15**. The untreated cells irradiated for ten minutes underwent an increase in temperature of <2 °C from 37.0 °C to 38.7 °C with 99.9 ± 1.1 % cell viability. Contrastingly, there was a large decline in cell viability of HeLa cells treated with the RGQDs and HA-GQDs with increasing irradiation time. Prior to irradiation, both samples had greater than 80% cell viability. For RGQDs, irradiation of ten minutes resulted in a measured final temperature of 43.5 ± 0.1 °C and 38.2 ± 4.3% cell viability. For HA-GQDs, ten minutes of laser irradiation resulted in a final measured temperature of 54.5 ± 0.3 °C and 22.9 ± 1.8 %.

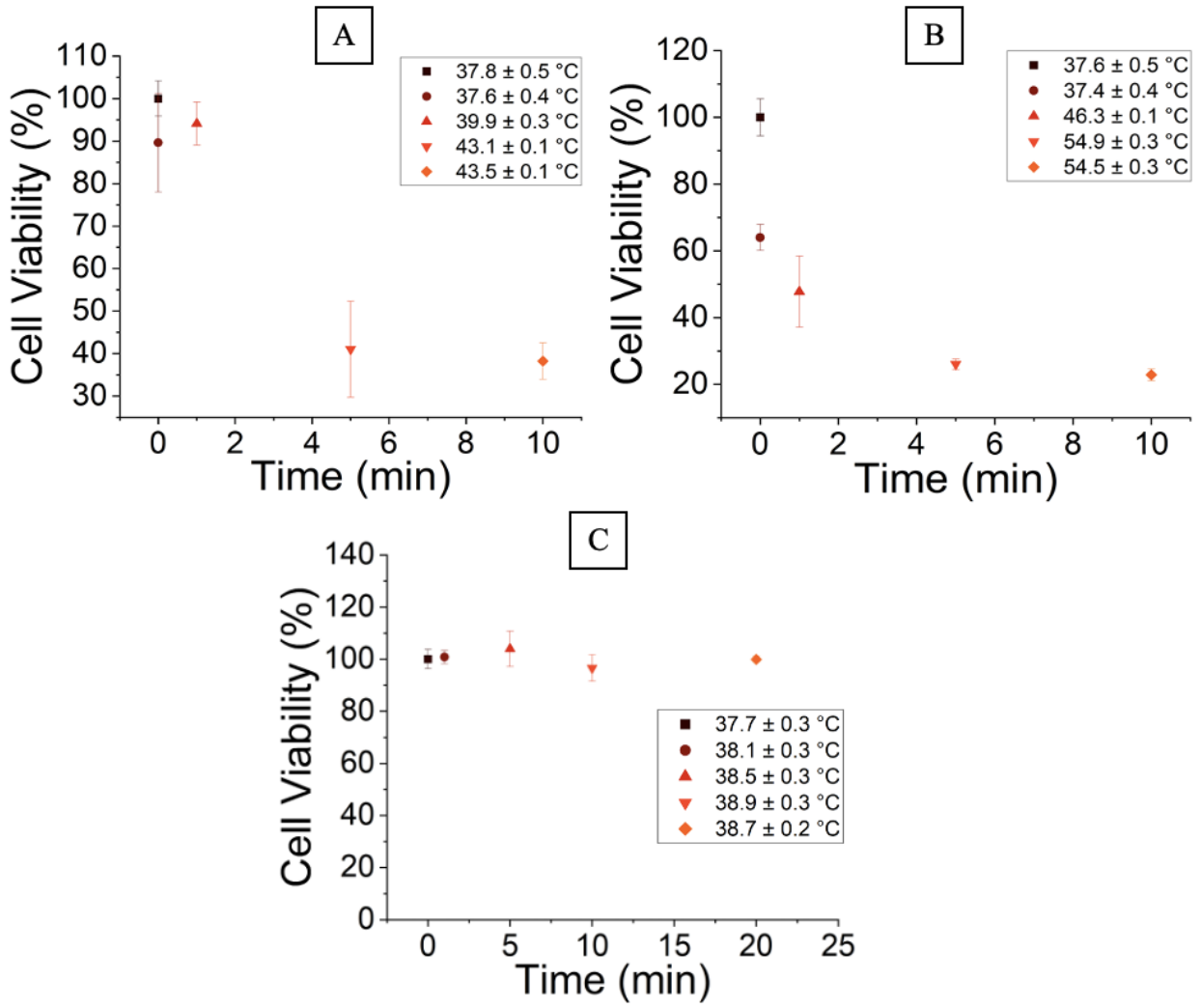

Figure 15. *In vitro* characterization of quantum dots as PTT agents. Results are shown for HeLa cells treated with aqueous solutions of (A) RGQDs (1.5 mg/mL) and (B) HA-GQDs (1.7 mg/mL) and irradiated for zero, one, five, and ten minutes. Following treatment with RGQDs and laser irradiation for ten minutes, the HeLa cells were at a measured final temperature of 43.5 ± 0.1 °C and only 38.2 ± 4.3% cell viability (A). For HA-GQDs, ten minutes of laser irradiation resulted in a final measured temperature of 54.5 ± 0.3 °C and only 22.9 ± 1.8 % (B). Cells untreated with graphene quantum dots were irradiated as a control for ten minutes (C). Following irradiation, the cells were at a temperature of 38.7 °C and had a viability of 99.9 ± 1.1%. This demonstrates that RGQDs and HA-GQDs can both be used as PTT agents to induce cell death.

Discussion

In this experiment, nanometer-sized GQDs were synthesized as photothermal agents via a top-down approach to give RGQDs and a bottom-up approach to give HA-GQDs. Both syntheses were simple and scalable, using two widely available precursor materials: reduced graphene oxide and hyaluronic acid. The two synthesized graphene quantum dot samples were characterized with TEM images and EDX spectroscopy. From the TEM images, both quantum dot samples had sizes

on the nanometer scale and resembled interatomic spacing of a graphene structure. As determined by EDX spectroscopy, the RGQDs had a higher level of functionalization with oxygen-containing functional groups (9.1% relative abundance of oxygen) than the HA-GQDs (1.9% relative abundance of oxygen). These characterization results of the two prepared samples support that graphene quantum dots were successfully synthesized via top-down and bottom-up methods.

The MTT assay results for each of these GQDs show that they are relatively biocompatible in HeLa cells, giving cell viabilities above 80% for treatment of cells with 1.5 mg/mL solutions for RGQDs and 1.7 mg/mL solutions for HA-GQDs. These concentrations represent a higher biocompatibility than most other carbon-based nanoparticle formulations. For example, one study on carbon nanotubes resulted with below 80% cell viability on MTT assays at concentrations of carbon nanotubes of 0.010 mg/mL.[36] Thus, these oxygen-functionalized graphene quantum dots may be more suitable as photothermal agents than other carbon-based nanoparticles based on their higher biocompatibilities. These concentrations (1.5 mg/mL for RGQDs and 1.7 mg/mL for HA-GQDs) were used in following experiments to characterize the potential of these materials as photothermal agents.

Aqueous solutions of RGQDs and HA-GQDs in a 37 °C environment were irradiated with an 808 nm laser. The temperature of the solutions was taken every fifteen seconds over a 45-minute period. During which time, the samples of RGQDs and HA-GQDs reached respective maximum temperatures of 47 and 46 °C. The DI water control had only a 0.5 °C change in temperature over 45 minutes of laser irradiation. Furthermore, both quantum dot formulations were photothermally stable after three cycles of laser excitation. This suggests that the quantum dots have high photothermal conversion efficiency and are stable upon irradiation. Thus, these quantum dot formulations can be used as photothermal agents to heat cancer cells to biologically detrimental temperatures upon laser irradiation.

Automated *in vitro* photothermal experiments using the graphene quantum dots as photothermal agents were performed using a retrofitted 3D-printer. There was a substantial decrease in cell viability for HeLa cells treated with the two solutions of GQDs and irradiated for ten minutes with a low power 808 nm laser. Cell viability was reduced to 38.2 ± 4.3% for cells treated with RGQDs (1.5 mg/mL) and 22.9 ± 1.8 % for cells treated with HA-GQDs (1.7 mg/mL). Trials run as controls—cells untreated with quantum dot formulations—resulted in 99.9% ± 1.1% cell viability following ten minutes of laser irradiation. This suggests that the laser alone is not capable of inducing appreciable levels of hyperthermia-induced cell death. Thus, for clinical applications of PTT, it is expected that the laser will not cause large amounts of off-target cell damage.

CONCLUSION

Photothermal therapy represents a possible avenue of cancer treatment with reduced side effects due to minimal damage to surrounding tissue. One large barrier to the transition of photothermal therapy to the clinic is the need for development of photothermal agents with low cytotoxicity and high photothermal conversion efficiency. RGQDs and HA-GQDs were successfully synthesized via top-down and bottom-up approaches. These quantum dots were determined to meet multiple criteria as effective photothermal therapy agents: the MTT assay results show they are biocompatible; the three rounds of oven experiments suggest photostability; and they showed high photothermal conversion efficiency with the temperatures measured following ten minutes of irradiation of GQD-treated cell cultures. *In vitro* characterization of these as photothermal agents resulted in cell viability reduced from above 80% to below 40% following one ten-minute laser irradiation treatment using near infrared light. These studies were successful in identifying RGQDs and HA-GQDs as possible candidates for photothermal agents with increased biocompatibility.

REFERENCES

1. Sung, H.; Ferlay, J.; Siegel, R. L.; Laversanne, M.; Soerjomataram, I.; Jemal, A.; Bray, F. Global Cancer Statistics 2020: GLOBOCAN Estimates of Incidence and Mortality Worldwide for 36 Cancers in 185 Countries. *CA Cancer J Clin* **2021**, *71* (3), 209-249. DOI: 10.3322/caac.21660.
2. Campbell, E.; Hasan, M. T.; Gonzalez Rodriguez, R.; Akkaraju, G. R.; Naumov, A. V. Doped Graphene Quantum Dots for Intracellular Multicolor Imaging and Cancer Detection. *ACS Biomater Sci Eng* **2019**, *5* (9), 4671-4682. DOI: 10.1021/acsbiomaterials.9b00603.
3. Liu, S.; Pan, X.; Liu, H. Two-Dimensional Nanomaterials for Photothermal Therapy. *Angew Chem Int Ed Engl* **2020**, *59* (15), 5890-5900. DOI: 10.1002/anie.201911477.
4. Baskar, R.; Lee, K. A.; Yeo, R.; Yeoh, K. W. Cancer and radiation therapy: current advances and future directions. *Int J Med Sci* **2012**, *9* (3), 193-199. DOI: 10.7150/ijms.3635.
5. Chapter 1 - Physics. In *Oral Radiology (Seventh Edition)*, White, S. C., Pharoah, M. J. Eds.; Mosby, 2014; pp 1-15.
6. Morgan, M. A. H., R. K.; Lawrence, T. S. . *Essentials of radiation therapy.* Oncohema Key., 2016. https://oncohemakey.com/essentials-of-radiation-therapy-4/. (accessed 2022 December 8).
7. Hobbie, R. K.; Roth, B. J. Medical Use of X Rays. In *Intermediate Physics for Medicine and Biology*, Hobbie, R. K., Roth, B. J. Eds.; Springer New York, 2007; pp 437-480.
8. Center, P. B. T. *What is proton therapy?* University of Tsukuba Hospital, https://www.pmrc.tsukuba.ac.jp/en/about_proton_therapy/pm.html (accessed 2022 December 8).
9. Torgovnick, A.; Schumacher, B. DNA repair mechanisms in cancer development and therapy. *Front Genet* **2015**, *6*, 157. DOI: 10.3389/fgene.2015.00157.
10. Hopkins, J. L.; Lan, L.; Zou, L. DNA repair defects in cancer and therapeutic opportunities. *Genes Dev* **2022**, *36* (5-6), 278-293. DOI: 10.1101/gad.349431.122.
11. Han, H. S.; Choi, K. Y. Advances in Nanomaterial-Mediated Photothermal Cancer Therapies: Toward Clinical Applications. *Biomedicines* **2021**, *9* (3). DOI: 10.3390/biomedicines9030305.
12. Zhou, J.; Lu, Z.; Zhu, X.; Wang, X.; Liao, Y.; Ma, Z.; Li, F. NIR photothermal therapy using polyaniline nanoparticles. *Biomaterials* **2013**, *34* (37), 9584-9592. DOI: 10.1016/j.biomaterials.2013.08.075.
13. Wang, S.; Ma, X.; Hong, X.; Cheng, Y.; Tian, Y.; Zhao, S.; Liu, W.; Tang, Y.; Zhao, R.; Song, L.; et al. Adjuvant Photothermal Therapy Inhibits Local Recurrences after Breast-

Conserving Surgery with Little Skin Damage. *ACS Nano* **2018**, *12* (1), 662-670. DOI: 10.1021/acsnano.7b07757.

14. Li, X.; Lovell, J. F.; Yoon, J.; Chen, X. Clinical development and potential of photothermal and photodynamic therapies for cancer. *Nature Reviews Clinical Oncology* **2020**, *17* (11), 657-674. DOI: 10.1038/s41571-020-0410-2.
15. Bommana, M. M.; Raut, S. Chapter 5 - Brain targeting of payload using mild magnetic field: Site specific delivery. In *Nanostructures for the Engineering of Cells, Tissues and Organs*, Grumezescu, A. M. Ed.; William Andrew Publishing, 2018; pp 167-185.
16. Maiti, D.; Tong, X.; Mou, X.; Yang, K. Carbon-Based Nanomaterials for Biomedical Applications: A Recent Study. *Front Pharmacol* **2018**, *9*, 1401. DOI: 10.3389/fphar.2018.01401.
17. Hasan, M. T.; Gonzalez-Rodriguez, R.; Lin, C.-W.; Campbell, E.; Vasireddy, S.; Tsedev, U.; Belcher, A. M.; Naumov, A. V. Rare-Earth Metal Ions Doped Graphene Quantum Dots for Near-IR In Vitro/In Vivo/Ex Vivo Imaging Applications. *Advanced Optical Materials* **2020**, *8* (21), 2000897. DOI: https://doi.org/10.1002/adom.202000897.
18. Cheng, C.; Li, S.; Thomas, A.; Kotov, N. A.; Haag, R. Functional Graphene Nanomaterials Based Architectures: Biointeractions, Fabrications, and Emerging Biological Applications. *Chem Rev* **2017**, *117* (3), 1826-1914. DOI: 10.1021/acs.chemrev.6b00520.
19. Iannazzo, D.; Pistone, A.; Celesti, C.; Triolo, C.; Patane, S.; Giofre, S. V.; Romeo, R.; Ziccarelli, I.; Mancuso, R.; Gabriele, B.; et al. A Smart Nanovector for Cancer Targeted Drug Delivery Based on Graphene Quantum Dots. *Nanomaterials (Basel)* **2019**, *9* (2). DOI: 10.3390/nano9020282.
20. Li, J.; Zhang, X.; Jiang, J.; Wang, Y.; Jiang, H.; Zhang, J.; Nie, X.; Liu, B. Systematic Assessment of the Toxicity and Potential Mechanism of Graphene Derivatives In Vitro and In Vivo. *Toxicol Sci* **2019**, *167* (1), 269-281. DOI: 10.1093/toxsci/kfy235.
21. Li, Z.; Fan, J.; Tong, C.; Zhou, H.; Wang, W.; Li, B.; Liu, B.; Wang, W. A smart drug-delivery nanosystem based on carboxylated graphene quantum dots for tumor-targeted chemotherapy. *Nanomedicine (Lond)* **2019**, *14* (15), 2011-2025. DOI: 10.2217/nnm-2018-0378.
22. Yan, Q.-L.; Gozin, M.; Zhao, F.-Q.; Cohen, A.; Pang, S.-P. Highly energetic compositions based on functionalized carbon nanomaterials. *Nanoscale* **2016**, *8* (9), 4799-4851. DOI: 10.1039/C5NR07855E.
23. Dash, B. S.; Jose, G.; Lu, Y.-J.; Chen, J.-P. Functionalized Reduced Graphene Oxide as a Versatile Tool for Cancer Therapy. *International journal of molecular sciences* **2021**, *22* (6), 2989. DOI: 10.3390/ijms22062989.

24. Mu, X.; Wu, X.; Zhang, T.; Go, D. B.; Luo, T. Thermal Transport in Graphene Oxide – From Ballistic Extreme to Amorphous Limit. *Scientific Reports* **2014**, *4* (1), 3909. DOI: 10.1038/srep03909.
25. Bhattacharjee, S.; Joshi, R.; Chughtai, A.; Macintyre, C. Graphene Modified Multifunctional Personal Protective Clothing. *Advanced Materials Interfaces* **2019**, *6*. DOI: 10.1002/admi.201900622.
26. Reed, M. A.; Randall, J. N.; Aggarwal, R. J.; Matyi, R. J.; Moore, T. M.; Wetsel, A. E. Observation of discrete electronic states in a zero-dimensional semiconductor nanostructure. *Physical Review Letters* **1988**, *60* (6), 535-537. DOI: 10.1103/PhysRevLett.60.535.
27. Thakur, M.; Kumawat, M. K.; Srivastava, R. Multifunctional graphene quantum dots for combined photothermal and photodynamic therapy coupled with cancer cell tracking applications. *RSC Advances* **2017**, *7* (9), 5251-5261. DOI: 10.1039/C6RA25976F.
28. Busch, P.; Heinonen, T.; Lahti, P. Heisenberg's uncertainty principle. *Physics reports* **2007**, *452* (6), 155-176. DOI: 10.1016/j.physrep.2007.05.006.
29. Hasan, M. T.; Lee, B. H.; Lin, C.-W.; McDonald-Boyer, A.; Gonzalez-Rodriguez, R.; Vasireddy, S.; Tsedev, U.; Coffer, J.; Belcher, A. M.; Naumov, A. V. Near-infrared emitting graphene quantum dots synthesized from reduced graphene oxide for in vitro/in vivo/ex vivo bioimaging applications. *2D Materials* **2021**, *8* (3), 035013. DOI: 10.1088/2053-1583/abe4e3.
30. Senbanjo, L. T.; Chellaiah, M. A. CD44: A Multifunctional Cell Surface Adhesion Receptor Is a Regulator of Progression and Metastasis of Cancer Cells. *Frontiers in Cell and Developmental Biology* **2017**, *5*, Mini Review. DOI: 10.3389/fcell.2017.00018.
31. Gupta, R. C.; Lall, R.; Srivastava, A.; Sinha, A. Hyaluronic Acid: Molecular Mechanisms and Therapeutic Trajectory. *Frontiers in veterinary science* **2019**, *6*, 192-192. DOI: 10.3389/fvets.2019.00192.
32. Sonia, T. A.; Sharma, C. P. 4 - Experimental techniques involved in the development of oral insulin carriers. In *Oral Delivery of Insulin*, Sonia, T. A., Sharma, C. P. Eds.; Woodhead Publishing, 2014; pp 169-217.
33. AnaPath. *Electron Microscopy*. August 11, 2022. anapath.ch/electron-microscopy-2/ (accessed 2022 December 8).
34. Colpan, C. O.; Nalbant, Y.; Ercelik, M. 4.28 Fundamentals of Fuel Cell Technologies. In *Comprehensive Energy Systems*, Dincer, I. Ed.; Elsevier, 2018; pp 1107-1130.
35. Baskin, Y.; Meyer, L. Lattice Constants of Graphite at Low Temperatures. *Physical Review* **1955**, *100* (2), 544-544. DOI: 10.1103/PhysRev.100.544.

36. Esfandiary, E.; Valiani, A.; Hashemibeni, B.; Moradi, I.; Narimani, M. The evaluation of toxicity of carbon nanotubes on the human adipose-derived-stem cells in-vitro. *Advanced biomedical research* **2014**, *3* (1), 40-40. DOI: 10.4103/2277-9175.125729.